

Microwave Negative Bursts as Indications of Reconnection between Eruptive Filaments and Large-Scale Coronal Magnetic Environment

Victor GRECHNEV¹, Irina KUZMENKO², Arkadiy URALOV¹, Ilya CHERTOK³, Alexey KOCHANOV¹

¹*Institute of Solar-Terrestrial Physics SB RAS, Lermontov St. 126A, Irkutsk 664033, Russia*

grechnev@iszf.irk.ru

²*Ussuriysk Astrophysical Observatory, Solnechnaya St. 21, Primorsky Krai, Gornotaezhnoe 692533, Russia*

kuzmenko_irina@mail.ru

³*Pushkov Institute of Terrestrial Magnetism, Ionosphere and Radio Wave Propagation (IZMIRAN), Troitsk, Moscow Region, 142190 Russia*

ichertok@izmiran.ru

(Received ; accepted)

Abstract

Low-temperature plasma ejected in solar eruptions can screen active regions as well as quiet solar areas. Absorption phenomena can be observed in microwaves as ‘negative bursts’ and in different spectral domains. We analyze two very different recent events with such phenomena and present an updated systematic view of solar events associated with negative bursts. Related filament eruptions can be normal, without essential changes of shape and magnetic configuration, and ‘anomalous’. The latter are characterized by disintegration of an eruptive filament and dispersal of its remnants as a cloud over a large part of solar disk. Such phenomena can be observed as giant depressions in the HeII 304 Å line. One of possible scenarios for an anomalous eruption is proposed in terms of reconnection of filament’s internal magnetic fields with external large-scale coronal surrounding.

Key words: filament eruptions; microwave negative bursts, Sun: coronal mass ejections (CMEs), Sun: radio radiation

1. Introduction

Depressions of the total microwave flux discovered by Covington & Dodson (1953) and called ‘negative bursts’ were interpreted by absorption in ejected filament material. Later studies (e.g., Tanaka & Kakinuma 1960) led to a general scenario of screening of a compact source (Sawyer 1977). The presumed association of microwave negative bursts with solar eruptions provides a basis for expectations to obtain additional information about eruptions and their parameters.

A multi-spectral study of the 2004 July 13 solar event has led Grechnev et al. (2008) to an unexpected conclusion about an anomalous course of the filament eruption in this event. Unlike a typical situation, the eruptive filament after the initial rise apparently disintegrated into a large cloud of fragments, which dispersed over almost a quarter of the visible solar disk, and then mostly descended on the solar surface far from the eruption site. The dispersed filament material screened the background solar emission. The 2004 July 13 eruptive event has shown that in addition to screening compact sources important can be screening large quiet Sun’s areas. The absorption phenomena were manifest in a microwave negative burst being especially pronounced in a HeII 304 Å image of SOHO/EIT (Delaboudinière et al. 1995) as a large darkening mismatching CME-related dimming observed in coronal extreme-ultraviolet (EUV) bands. Among all of EUV emission lines, in which observations are carried

out, the HeII 304 Å line is best suited for studies of prominences and filaments due to its temperature sensitivity range (maximum at 80 000 K). SOHO/EIT produced HeII 304 Å images usually once in 6 hours.

We have not found in the literature descriptions of similar phenomena, except for the only report on the 2003 November 18 event (Slemzin et al. 2004; Grechnev et al. 2005), of which we were aware (V.G. and I.C. were among the co-authors). A negative burst could not be observed in this event due to subsequent flaring. The event was studied in detail later (Grechnev et al. 2013). A review of Gilbert et al. (2007) does not mention such phenomena. A reason why anomalous eruptions were not well known previously seems to be clear. Observations of eruptions in the H α line are limited by the Doppler shift, which rapidly removes absorbing features from the filter passband even with moderate line-of-sight velocities. Observations in the HeII 304 Å line were infrequent in the past.

Proceeding from the results of Grechnev et al. (2008), we searched for i) events with negative microwave bursts recorded in Nobeyama and Ussuriysk, and ii) events, in which large darkenings were observed in 304 Å images. One more event with anomalous eruption, which occurred on 1998 April 29 around 17:30 UT, was revealed from EIT data (Chertok & Grechnev 2003) and analyzed by Grechnev et al. (2011a).

The events with negative bursts recorded at several frequencies were analyzed by using a simple model developed for estimating parameters of ejected material. The model

allows one to calculate the spectrum of the total solar radio flux by considering contributions from the chromosphere, a screen constituted by material of an eruptive filament ‘inserted’ into the corona at some height, and coronal layers both between the chromosphere and the screen, and between the screen and the observer (Grechnev et al. 2008). By comparing the frequency distribution of the microwave absorption depth in an observed negative burst with an absorption spectrum simulated with the model, it is possible to estimate the kinetic temperature of the screen, its optical thickness at each frequency, the area, and the height above the chromosphere. Actual fluxes of compact sources were measured from NoRH images and used among other input parameters of the model in the simulations.

The studies of Grechnev et al. (2008; 2011a) and Kuzmenko et al. (2009) presented several events with negative bursts detected mostly from measurements with NoRP and RT-2 (2.8 GHz) in Ussuriysk (Kuzmenko et al. 2008) and some events with a large darkening in 304 Å images. The estimated parameters are consistent with the assumption about screening of the solar emission by cool material of an eruptive filament. Among these events, there were also those with anomalous eruptions. Grechnev et al. (2008) concluded that magnetic reconnection was most likely implicated in the observed transformation of the eruptive filament, but a particular role of reconnection and a possible scenario of such an anomalous eruption remained unclear.

Noticeable negative bursts were recently observed in two very different events. The 2011 June 7 event was associated with a powerful flare and strong impulsive microwave burst. The 2011 December 13 event has not produced any detectable enhancement in total flux records. We firstly analyze the two recent events. Then we present a possible scenario of an anomalous eruption and discuss distinctive particularities and possible common properties of such events. On the basis of these considerations and results of previous studies we endeavor to supplement a systematic view of solar eruptions associated with negative bursts.

2. Recent Events with Negative Bursts

Our analysis of events with microwave negative bursts uses total flux measurements at several frequencies routinely carried out with the following instruments:

- the Nobeyama Radio Polarimeters (NoRP, Torii et al. 1979; Nakajima et al. 1985); we use data at the frequencies of 1, 2, 3.75, 9.4, and 17 GHz;
- the radiometers of the Learmont station of the USAF RSTN network; we use data at the frequencies of 1.4, 2.7, 5.0, and 8.8 GHz;
- the RT-2 radiometer observing at 2.8 GHz (Kuzmenko et al. 2008) operated by the Ussuriysk Astrophysical Observatory (station code ‘VORO’).

Parameters of quasi-stationary microwave sources were measured from images produced by the Nobeyama

Radioheliograph (NoRH, Nakajima et al. 1994) at a frequency of 17 GHz. Eruptive events were analyzed by using EUV images produced by SOHO/EIT (Delaboudinière et al. 1995), STEREO/EUVI (Howard et al. 2008), and SDO/AIA (Lemen et al. 2012) as well as NoRH images as long as they were available. We also used the images produced with the Siberian Solar Radio Telescope at 5.7 GHz (SSRT, Smolkov et al. 1986; Grechnev et al. 2003).

2.1. Event I: 2011 December 13

On 2011 December 13, an isolated negative burst was observed. Unlike a typical situation, it was not preceded by a flare burst. A possible enhancement of the soft X-ray flux was inconspicuous in GOES plots. Figure 1a presents the total flux time profiles of the microwave emission with subtracted pre-burst levels, normalized to the quiet Sun’s total flux at each frequency, and smoothed over 30 s. As Figure 2a–d shows, depression of the microwave emission was caused by screening remote compact sources by a steadily expanding quiescent filament. The eruptive filament was observed as a moving dark feature covering the remote sources on the limb both in NoRH 17 GHz and SDO/AIA 304 Å images. The fluxes of the screened compact sources estimated from the 17 GHz NoRH image at 01:10 were ≈ 4 sfu. The positions of the screened sources are shown by the white contours in Figure 2d.

The difference SDO/AIA 304 Å image in Figure 2d shows at 01:10 the area of the darkening at a level of -20% of the brightness to be 0.5% of the solar disk. The maximum depth of the depression reached -54% . The eruptive filament was also observed from the vantage point of STEREO-A 110° west of the Earth. The STEREO-A/EUVI 304 Å image in Figure 2e allows us to estimate the geometrical depth of the eruptive filament $L \approx 100$ Mm in the direction close to the line of sight of an observer on Earth.

With these quantities, parameters of the screen were estimated from the model simulations of the absorption spectrum. The estimated temperature of the filament material is 10 000 K. The estimated area is about twice larger than the 304 Å image shows. This is possible, because the body of the filament conspicuous in Figure 2e can be surrounded by a sheath invisible at 304 Å but contributing to microwaves. The estimated mass of the filament of 3×10^{14} g is less than those provided by estimations in other events (see Table 1), but still comparable with typical masses of filaments.

Eruption of the filament far from active regions determined weakness of the emission from the post-eruption arcade, although the arcade was detectable, e.g., in 304 Å images in Figure 2d,e. Weakness of the arcade emission determined the absence of a detectable burst in total flux records before the negative burst. This weak eruptive event has produced a CME visible in a SOHO/LASCO/C2 image in Figure 2f. Properties of the 2011 December 13 event appear to be typical of non-flare-related eruptions (Chertok et al. 2009). Among these properties is gradual acceleration of the CME in LASCO/C2 images according to a height-time plot in the SOHO LASCO CME

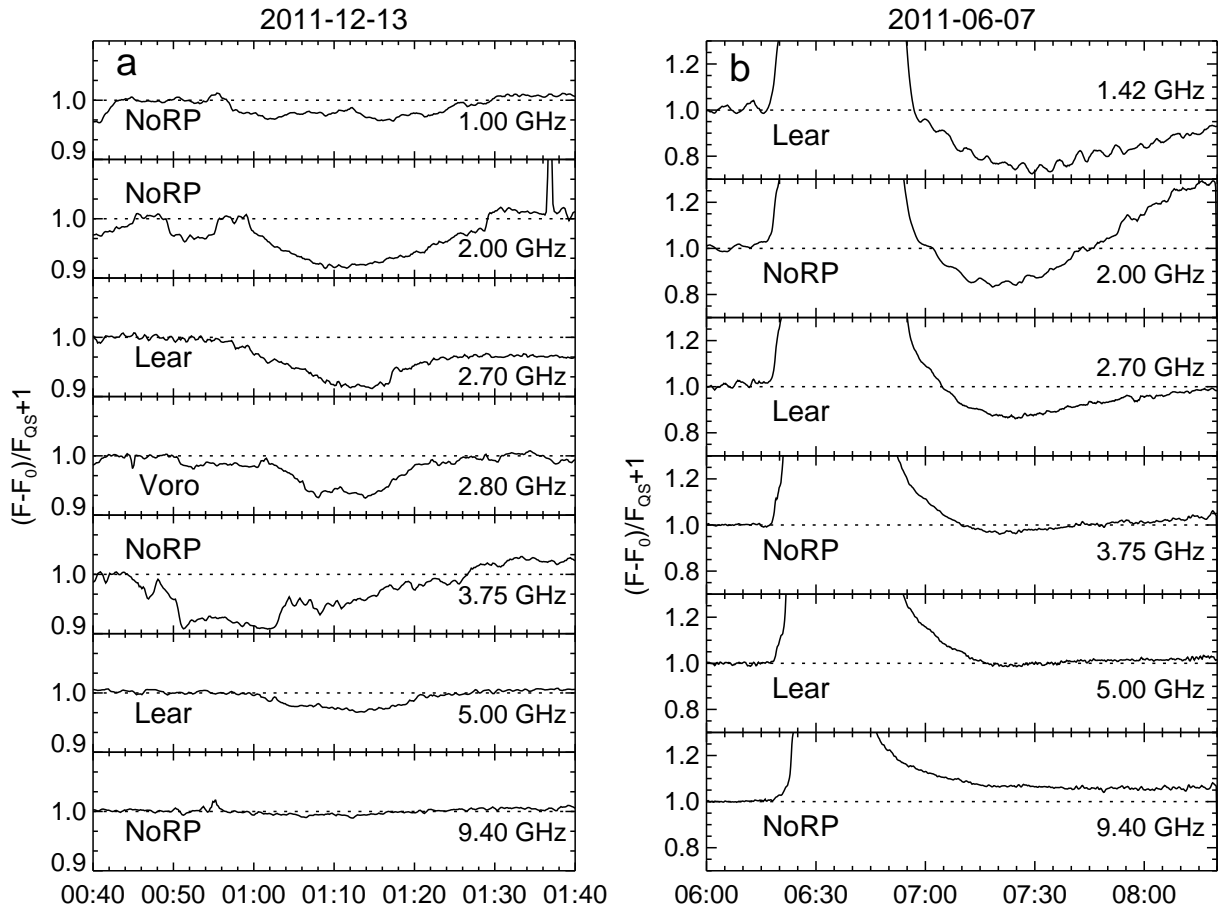


Fig. 1. Negative bursts recorded on 2011 December 13 (a) and on 2011 June 7 (b). Time profiles are normalized to the quiet Sun's levels at different frequencies.

Catalog (<http://cdaw.gsfc.nasa.gov/CMElist>, Yashiro et al. 2004). Finally we note that the 2011 December 13 eruption and negative burst resemble the event discussed by Maksimov & Nefedev (1991), which also occurred according to the ‘classical’ screening scenario (Sawyer 1977).

2.2. Event II: 2011 June 7

The 2011 June 7 event occurred in active region 11226 (S22 W64, β -configuration). Images produced before the event in the Big Bear Solar Observatory in the $H\alpha$ line show a small filament in the active region. The pre-eruptive filament is also visible in SDO/AIA 304 Å images. The filament started to rise by 06:11. The related flare of M2.5 GOES importance started at 06:16.

Importance of this event for our study is determined by an anomalous eruption, which was the most demonstrative one ever observed. The eruptive filament after the initial lift-off by 06:25 apparently disintegrated into a huge dome of jet-like fragments, most of which turned back to the solar surface and produced a ‘coronal rain’, which went on four hours. Absorbing fragments of the dispersed filament are well visible not only at 304 Å, but even in non-subtracted images at 193 Å in Figure 3a and in other coronal lines up to 94 Å (see also 211 Å images

in Figure 8).

The SDO/AIA 304 Å difference image in Figure 3b shows a large darkening, while some portion of the area subjected to the coronal rain was bright. The area of the darkening at a level of the brightness decrease of -25% reached 6.5% of the solar disk. The deepest local depression reached -90% . The large brightening area (2.7% of the solar disk) indicates the presence of hotter material there. The total area occupied by manifestations of dispersed filament material was 6.6% from SDO/AIA images and 8% from the STEREO-A/EUVI 304 Å image in Figure 3c.

NoRH recorded the 2011 June 7 event by the end of the observations at 06:30. The negative burst began after 06:50. For this event microwave images produced with SSRT at a frequency of 5.7 GHz are available. Figure 4a shows a pre-event SSRT image averaged over several frames observed from 04:00 to 07:00. Figures 4b and 4c show the Sun observed during the negative burst. Dark portions of a disk in the right part of the images are due to adjacent negative interference beams of the SSRT that limit the field of view. To emphasize low-brightness features of interest, we had to limit bright sources from above (their brightness temperatures exceed 1.7×10^5 K)

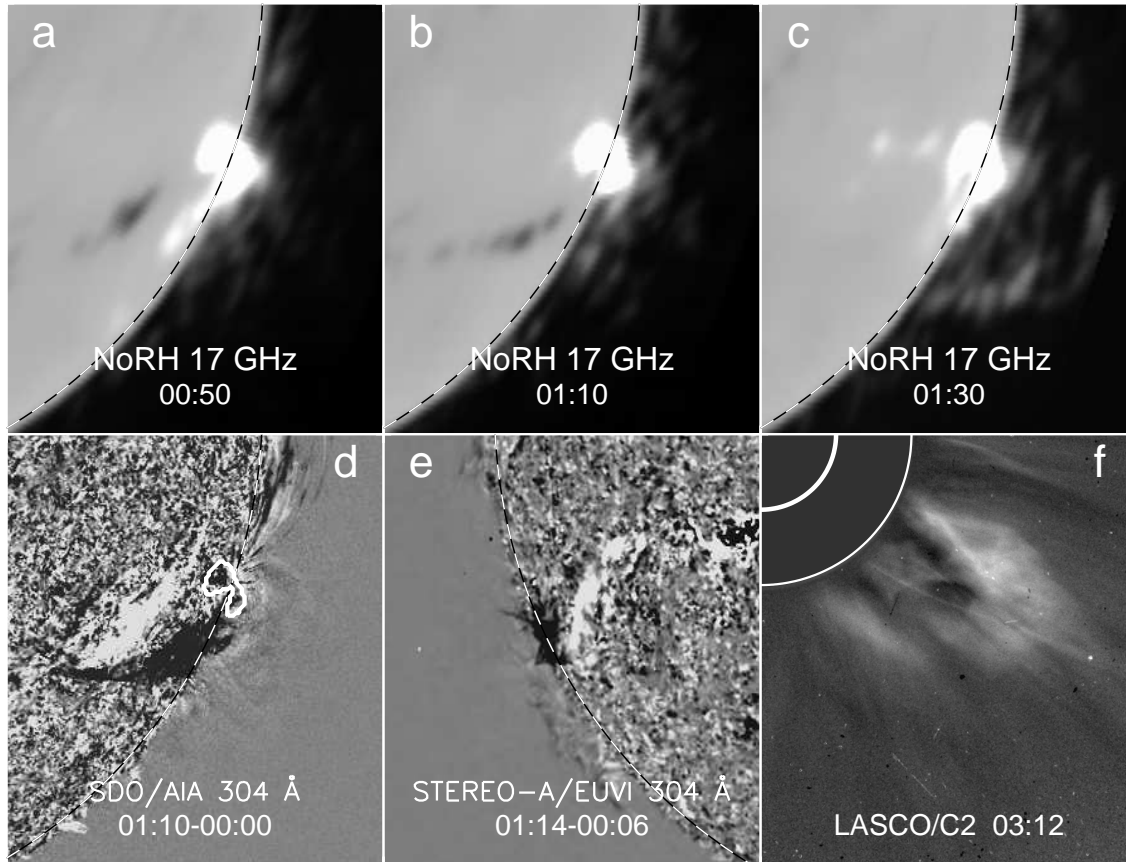


Fig. 2. Filament eruption on 2011 December 13: a-c) microwave NoRH images without subtraction, d) SDO/AIA and e) STEREO-A/EUVI difference images at 304 Å, e) LASCO/C2 ratio image. The white contours in panel (d) outline the screened sources in the NoRH 17 GHz image. The dashed circle denotes the solar limb. The white solid circles in panel (f) denote the solar limb and the inner boundary of the LASCO/C2 field of view.

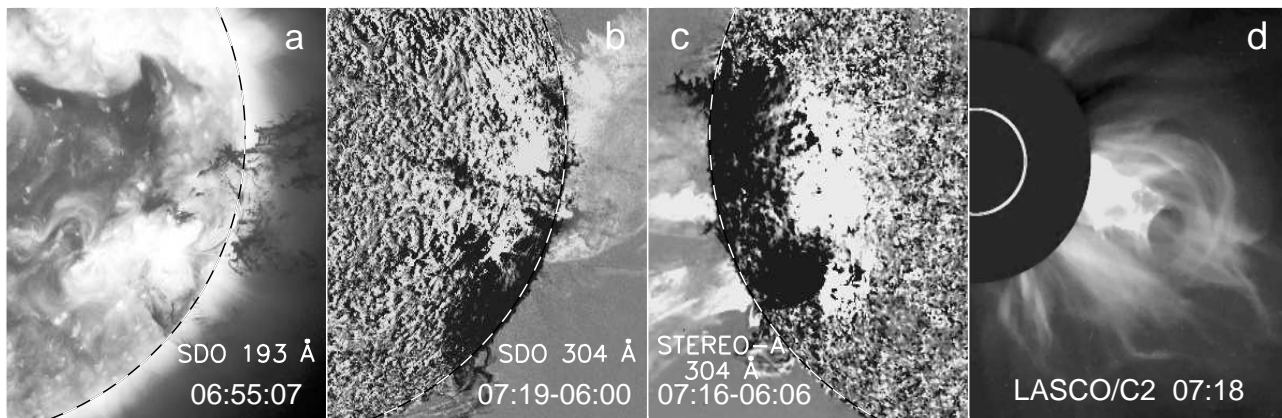


Fig. 3. 2011 June 7 event: SDO/AIA image at 193 Å (a), SDO and STEREO-A differences at 304 Å (b,c), SOHO/LASCO/C2 image of the CME (d). The dashed circle denotes the solar limb.

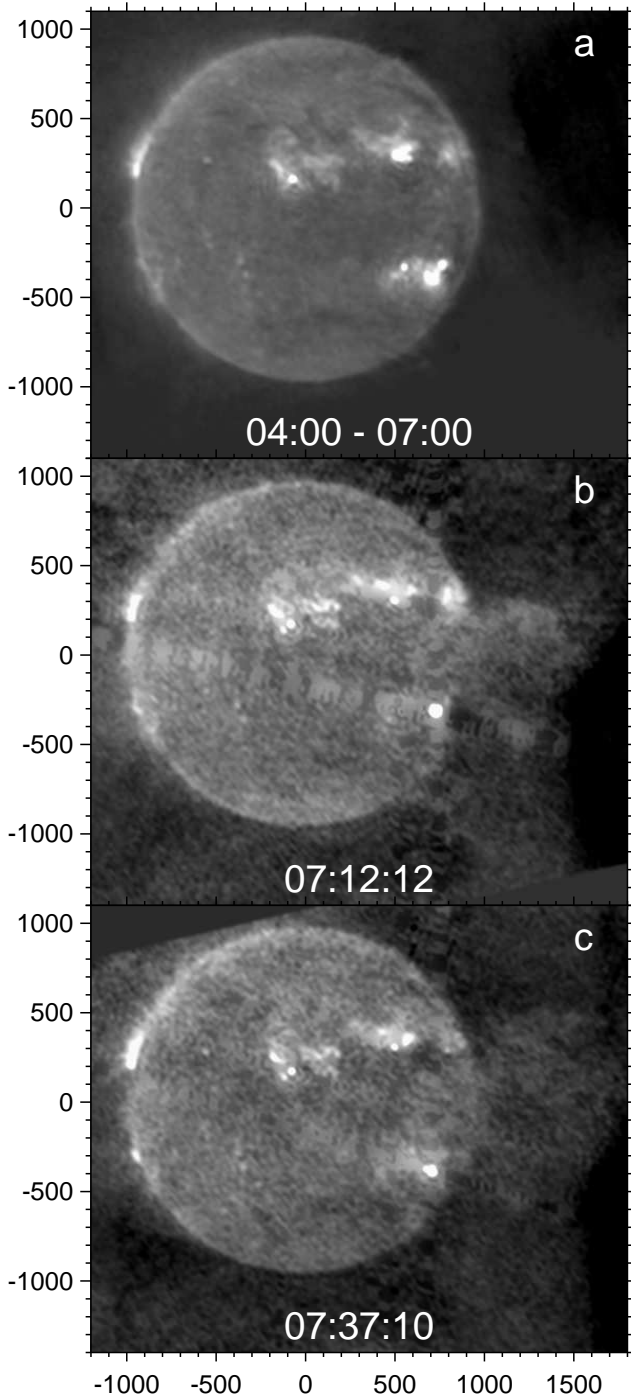


Fig. 4. SSRT observations on 2011 June 7 at 5.7 GHz: a) pre-event image averaged from 04:00 to 07:00; b, c) a huge cloud of dispersed filament material expanding above the west limb. The axes show hereafter arc seconds from the solar disk center.

which produces impression of their saturation.

The 5.7 GHz SSRT images in Figures 4b and 4c present a huge cloud consisting of dispersed filament material above the limb and, possibly, partially on the solar disk. Inevitable residual side lobes still remaining after the CLEAN routine (long fringe-like stripes crossing bright

sources) somewhat distort the image. A gradual expansion of the cloud is visible in the two lower panels.

The cloud is visible in microwaves undoubtedly due to thermal free-free emission. The optical thickness of the cloud can be less than in EUV so that the microwave brightness responds to emissions from different depths averaged along the line of sight. If the optical thickness is large, then the microwave brightness temperature is equal to the kinetic temperature of a source. Bright parts of the cloud are similar in brightness to the quiet Sun, whose brightness temperature is 16 000 K at 5.7 GHz. Thus, bright portions of the cloud had an average temperature of $\gtrsim 16\,000$ K, which suggests appreciable heating of dispersed filament material. A reason for a darker appearance of the middle part of the cloud is difficult to understand from a single-frequency image. This can be due to either a lower temperature or a lesser thickness.

This event is the only one of such a kind observed with SSRT so far. Analysis of other events in which negative bursts were observed has shown that the expected depression depth at the relatively high frequency of 5.7 GHz was less than the sensitivity of SSRT (Grechnev et al. 2011a).

A negative burst was observed after the impulsive burst at frequencies below 5 GHz. Figure 1b shows the negative burst with the pre-burst levels subtracted from the time profiles, normalized to the quiet Sun, and smoothed over 30 s like Figure 1a. As observations and model simulations show, the negative burst in this event was due to screening both a compact source and a large quiet Sun’s area. Since the negative burst occurred after completion of NoRH observations, we use in our modeling the flux of the screened compact radio source of ≈ 3 sfu measured from a NoRH 17 GHz image at 06:00. The mass of absorbing material estimated from the radio spectrum is 6×10^{15} g. The estimated average temperature is higher than that in the preceding event, 3×10^4 K, which seems to be consistent with the presence of large brightening areas in Figure 3b,c. The temperature is consistent with the estimate from the SSRT data. The area of the absorbing cloud estimated from model simulations is almost twice larger than that estimated from the 304 Å images. Note, however, that the model used in the estimations takes account of the on-disk projection of the screening material and does not consider an exotic possibility of a sporadic “another Sun” constituted by the huge microwave-emitting cloud, and therefore the estimates for this event are less reliable.

The top part of the filament, which was initially dark, then brightened up in the course of its lift-off, while trailing material remained predominantly dark. Approximate estimates of kinematics of the leading filament’s edge have provided its initial velocity (06:10–06:20) in the plane of the sky of about 17 km s^{-1} . By 06:24 the filament accelerated up to 540 km s^{-1} and then started to decelerate. After 06:34 the bright top of the eruption reached the edge of the field of view of SDO/AIA that does not allow us to estimate its final velocity. The last measurement provides 214 km s^{-1} for the leading edge. The trailing dark portion also showed the highest speed between 06:25 and 06:30 and decelerated later on.

The sharp filament eruption with strong acceleration followed by deceleration must have produced a shock wave via the impulsive-piston mechanism (see Grechnev et al. 2011b). This expectation is confirmed by observation of an ‘EUV wave’ in the 193 Å channel starting from 06:24 and a type II radio burst (Learmonth).

A fast CME was observed after the eruption. The CME in Figure 3d resembles in shape the cross section of a semi-torus with its straight poloidal axis being close to the plane of the sky so that its circular toroidal axis is close to the line of sight. Brighter features suggestive of remnants of filament material are visible near the bottom of the central tube of the torus (cf. Figure 6d,e,f). LASCO/C2 movies available in the SOHO LASCO CME Catalog show at 09:30–11:30 that some pieces of bright material reached heights of $(2-2.5)R_{\odot}$ above the solar surface and then fell back.

3. Discussion

3.1. Revealed Events

Information about microwave negative bursts in the past years is contained in reports on single-frequency observations of solar radio bursts presented in the *Solar-Geophysical Data* bulletin issued from 1955 to 2009. Overview of reported events with negative bursts (code ‘ABS’) contained in *Solar-Geophysical Data* shows their very rare occurrence. Figure 5 summarizes the yearly number of the reports since 1991 (when observations in Ussuriysk started) and up to 2009. Multiple reports on the same event have been removed. The shaded histogram selects only those events which could be observed in Nobeyama or Ussuriysk. The total number of negative bursts reported in 1991–2009 within the observational daytimes in Nobeyama and Ussuriysk was as small as 22. A detailed analysis of such events has become possible when EUV observations have become available, i.e., when SOHO was launched (the dashed vertical line in Figure 5). The rate of yearly reported events mainly corresponds to the progression of the solar cycle, which can be expected.

Table 1 lists characteristics of revealed negative bursts (including two events considered in the preceding section and two most recent events which have not yet been analyzed) and estimated parameters of absorbing material. The dates and times are related to the deepest depression. Column 4 presents a range of durations observed at different frequencies (typically longer at lower frequencies). The depth in column 5 corresponds to a deepest depression expressed as a percentage of the quiet Sun’s total flux. Column 6 specifies a frequency at which the deepest depression occurred. As column 10 of Table 1 shows, more than 50% of the revealed event were not registered in *Solar-Geophysical Data*. Even if the missed events were included into the histogram in Figure 5, the total number of events with negative bursts would remain small.

Analysis of several events has led Grechnev et al. (2008; 2011a) and Kuzmenko et al. (2009) to the following conclusions. Screening both compact sources and large quiet Sun’s areas can be important. Negative bursts are

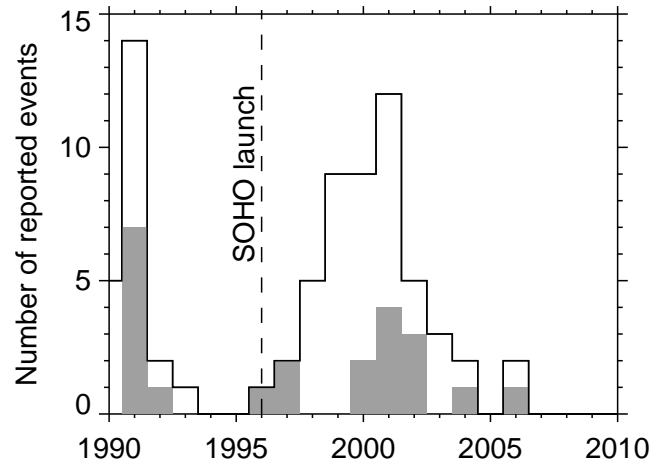


Fig. 5. Yearly occurrence of negative bursts in 1991–2010 according to all reports in *Solar-Geophysical Data* (solid histogram) and during the observational daytime in Nobeyama and Ussuriysk (shaded bars). The vertical dashed line marks the date of SOHO launch.

best observed at 1–5 GHz, where the corona is optically thin and contrast of ejecta against the quiet Sun is sufficient. Nevertheless, absorption sometimes appears at 17 GHz. A post-burst decrease can be observed if a preceding flare is short and no bursts occur afterwards. When negative bursts occur, large darkening can appear at 304 Å mismatching CME-related dimming in coronal bands.

In all events screening of both compact sources and considerable quiet Sun’s areas occurred. Almost all negative bursts in the analyzed events had a type of ‘post-burst decrease’ and resulted from the eruption of a filament from an active region. An impulsive non-thermal burst is typically observed before a negative burst, because eruptions in strong magnetic fields of active regions cause strong gyrosynchrotron emission. If the eruption of a filament occurs out of active regions where magnetic fields are weak, the enhancement of the microwave emission is predominantly thermal and weak. In such a case, no pronounced increase of the emission in total flux records is expected. If a non-flare-related eruptive filament screens a compact radio source, then an isolated negative burst is possible as was the case in the 2011 December 13 event.

Two scenarios of screening have been revealed. In the first scenario, which occurs in the majority of events, the shape and structure of an eruptive filament persist. Such an expanding filament moves away from the solar surface without dramatic losses of mass and looks like a moving screen with increasing size and decreasing opacity. Occasionally eruptions develop in anomalous way. The eruptive filament essentially changes, while a part of its material disperses over a large area and descends far from the eruption site.

3.2. Anomalous Eruptions

The 1998 April 29 event with a huge darkening in an EIT 304 Å image mismatching dimmings observed in coronal lines was presented by Chertok & Grechnev (2003).

Table 1. Summary of revealed events with negative bursts

No.	Date	Time	Duration min	Depth %	ν GHz	T_S K	A_S/A_\odot %	M 10^{14} g	SGD report	Remarks
1	2	3	4	5	6	7	8	9	10	11
1	1998-04-29	17:29	53–65	11	2.8				Yes	anomalous
2	2000-06-16	00:10	28–80	19	1.0	9000	6.0	13	No	
3	2002-02-06	04:51	18–34	10	2.0	9000	3.5	20	Yes	
4	2002-02-07	01:10	16–32	10	2.0	11000	4.0	15	No	
5	2002-06-02	00:01	22–26	6	2.7	8000	2.0	9	Yes	
6	2003-05-28	00:10	10						No	onset only
7	2004-07-13	00:55	37–80	12	1–2.8	10000	6.4	15	No	anomalous
8	2005-01-01	01:06	45–65	13	2.0	14000	5.0	20	No	
9	2010-11-12	01:55	~ 25	2	1.0				–	
10	2011-06-07	07:20	30–100	25	1.4	30000*	15*	60*	–	anomalous
11	2011-12-13	01:14	20–31	8	2.0	10000	1.2	3	–	isolated
12	2012-01-12	01:26	37–56	6	2.0				–	
13	2013-02-06	00:43	15–45	12	2.0				–	

*Estimated parameters are questionable due to exceptional characteristics of the ejected cloud

Initially this event was not recognized as an anomalous eruption, which were unknown at that time. A negative burst was recorded in Penticton. An anomalous eruption in this event was revealed later (Grechnev et al. 2011a).

The first well-studied anomalous eruption of a filament from an active region occurred on 2004 July 13 (Grechnev et al. 2008). The ejecta disintegrated into two parts, one of which flew away as a decelerating CME, and another part returned to the Sun and descended far from the eruption center. The latter part absorbed background solar emission in various spectral ranges that was observed as a negative microwave burst, widespread faint moving dimmings at 195 Å, and a huge dimming at 304 Å, as Figure 7 shows in the middle row. An ‘EUV wave’ is visible in Figure 7f. The area of the 304 Å darkening at a level of -25% was 6.7% of the solar disk.

NoRH 17 GHz images reveal a dark moving blob, which is outlined with the white circle in Figure 7 (top row). Its lowest brightness temperatures reached 6000–8000 K against the background of the quiet Sun (10000 K at 17 GHz) indicating its large optical thickness and, consequently, the kinetic temperature of ~ 6000 K. For comparison, the estimated average temperatures of absorbers in Table 1 are typically $\sim 10^4$ K. This blob probably showed a densest piece of dispersed filament material.

The events of 2004 July 13 and 2011 June 7 appear to be similar. On 2011 June 7, dark filament fragments were visible even in original non-subtracted images in all coronal channels up to 94 Å. Such strong absorption was observed for the first time. Grechnev et al. (2011a) contemplated probable properties of events with anomalous eruptions. The 2011 June 7 event exhibited most of these properties indeed. The event was accompanied by a powerful flare, ‘EUV wave’, and type II radio burst. The authors anticipated higher probability for an anomalous course of an eruption if it occurred in a complex magnetic configuration, which was really the case in the 2011 June 7 event. By contrast, the eruption on 2011 December 13

occurred outside of active regions, and its course was not anomalous in accordance with expectations.

3.3. A Possible Scenario for an Anomalous Eruption

Gilbert et al. (2007) consider a few types of filament eruption based on the traditional conception of a filament as a dense lower part of a large-scale magnetic rope. Eruptions of filaments are divided into three types: full eruptions, partial, and failed ones. The type of an eruption is considered to be determined by the position of the reconnection site relative to the filament (below the filament, within its limits, or above it). If filament material falls back on the Sun, then its returning trajectory is considered to be the same as that of its lift-off. A possibility of reconnection between magnetic structures of an eruptive filament and surrounding magnetic fields in the corona was not considered by the authors. However, decay of the magnetic structure of an eruptive filament is possible in some events due to such reconnection processes. The filament loses integrity in such a situation.

Figure 6 presents a possible scenario for an anomalous eruption of an inverse filament in a quadrupole configuration. We consider an apex cross section of a three-dimensional toroidal magnetic flux rope with ends rooted in the photosphere. Such a toroidal flux rope is well visible in the LASCO/C2 image of the 2011 June 7 CME in Figure 3d. The initial filament in Figure 6a (time of t_1) is in the equilibrium state. The dashed lines present the initial separatrices. Let us follow evolution of plasma within the gray ring cross section of the flux rope.

An upward rise of the flux rope leads to magnetic field stretching, and a vertical current sheet develops. Standard flare reconnection starts. With the flare onset (t_2 in Figure 6b), separatrices *AA* and *BB* approach. In the course of reconnection, the flux rope acquires additional rings of the poloidal magnetic field, which creates a progressively increasing propelling force. Acceleration of the expanding flux rope increases. The flux rope exits into

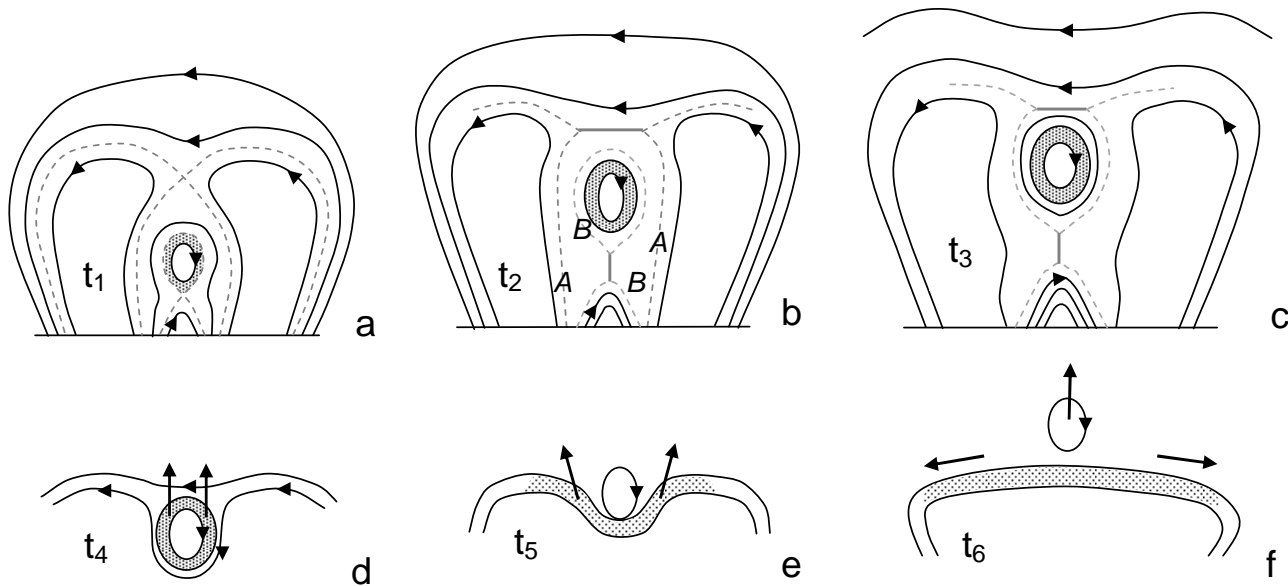


Fig. 6. A possible scenario of an anomalous eruption of an inverse filament in a quadrupole configuration.

the outer domain (t_3 in Figure 6c). By this moment, separatrices AA and BB have already merged. A horizontal current sheet forms, and reconnection with the external magnetic field starts to ‘undress’ the flux rope thus making the gray ring portion of interest naked. The poloidal flux starts to decrease. Plasma of the filament is dispersed over the solar surface (Figure 6d–f). The ‘undressing’ of the gray ring portion and its heating goes on in reconnection with external magnetic fields ($t_4 - t_5$). The newly formed magnetic tube straightens and becomes a static magnetic loop. The plasma upflow ceases (Figure 6f). The sideways velocity of plasmas flowing from the top is almost equal to the upwards velocity of the ejecta. The process results in dispersal over a large area of material, which was previously confined within the ring cross section.

Note that blow of a fast and dense plasma downflow should produce a shock in the transition region. Observations of two anomalous eruptions confirm this expectation indeed. Figure 7k–o (bottom row) shows $H\alpha$ ratio images produced with the Polarimeter for Inner Coronal Studies (PICS) of the Mauna Loa Solar Observatory (MLSO). Transient remote brightenings produced by falling fragments of the former filament are indicated by the arrows in these images. Similar transient brightenings obviously caused by downstream dark material are visible in Figure 8, which presents SDO/AIA 211 Å images (temperature sensitivity maximum 2 MK) of the 2011 June 7 event. These brightenings are visible in all coronal channels of AIA up to 94 Å and in the 1600 Å channel. Such remote non-active-region brightenings in the chromosphere were interpreted many years ago by Hyder (1967a; 1967b) as the places of dissipation of kinetic energy of falling filament material.

In the considered scenario, reconnection with external magnetic field in the course of ‘undressing’ of the flux

rope tends to increase its velocity due to upwards magnetic tension of reconnected field lines (Figure 6d,e), while the decrease of the poloidal flux results in a decrease of the total propelling force. The retarding influence of the toroidal flux’s tension and gravity persists. The scenario predicts that the flux rope should sharply accelerate and then gradually decelerate. This was really the case in the 2011 June 7 event. Similarly, all observed moving features only decelerated in the 2004 July 13 event (Grechnev et al. 2008).

4. Concluding Remarks

Despite the rare occurrence of negative bursts, their studies have provided new insight into solar eruptions. An important condition of reaching success in these studies was a combined analysis of microwave total flux and imaging data provided mainly by NoRP and NoRH along with EUV images. These studies have revealed:

- different kinds of negative bursts ranging from the well-known post-burst decrease up to unusual isolated negative bursts without preceding flare bursts;
- negative bursts caused by screening not only compact sources, but also large quiet-Sun areas;
- absorption of the background emission in material of an eruptive filament, which can also be observed as a depression of the HeII 304 Å line emission, usually without pronounced counterparts in EUV emission lines;
- two scenarios of screening by either a steadily expanding filament or remnants of a filament dispersed in an anomalous eruption;
- anomalous eruptions and their expected properties, which have been inferred from scarce data of past years and were confirmed by recent observations.

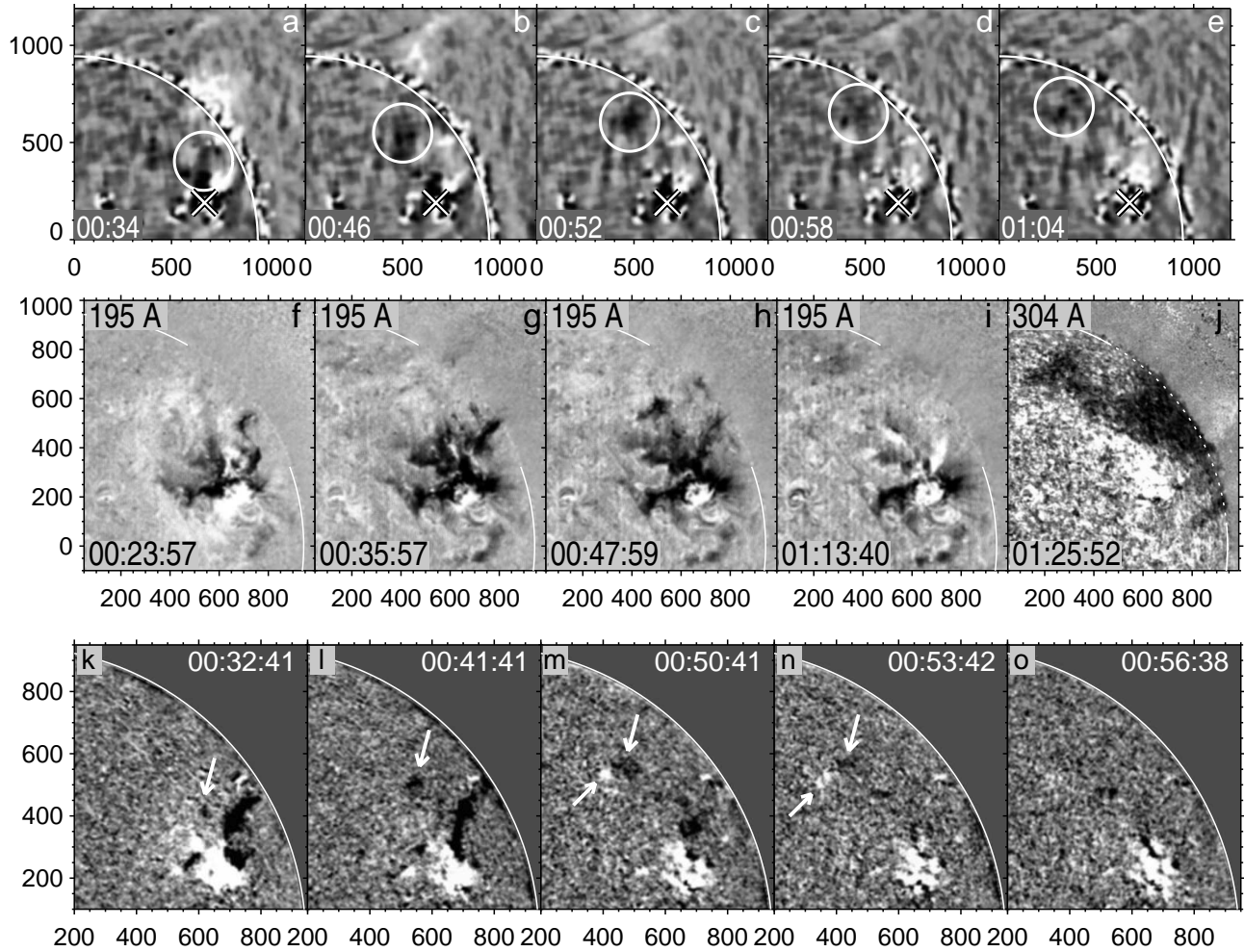


Fig. 7. Anomalous eruption on 2004 July 13. a–e) Moving dark absorbing feature (white circle) in NoRH 17 GHz difference images. The slanted cross marks the eruption center. f–j) SOHO/EIT ratio images at 195 Å and 304 Å. k–o) H α ratio images (PICS, MLSO). The arrows indicate a dark moving fragment of the disintegrated filament and remote brightenings. The white arcs denote the solar limb.

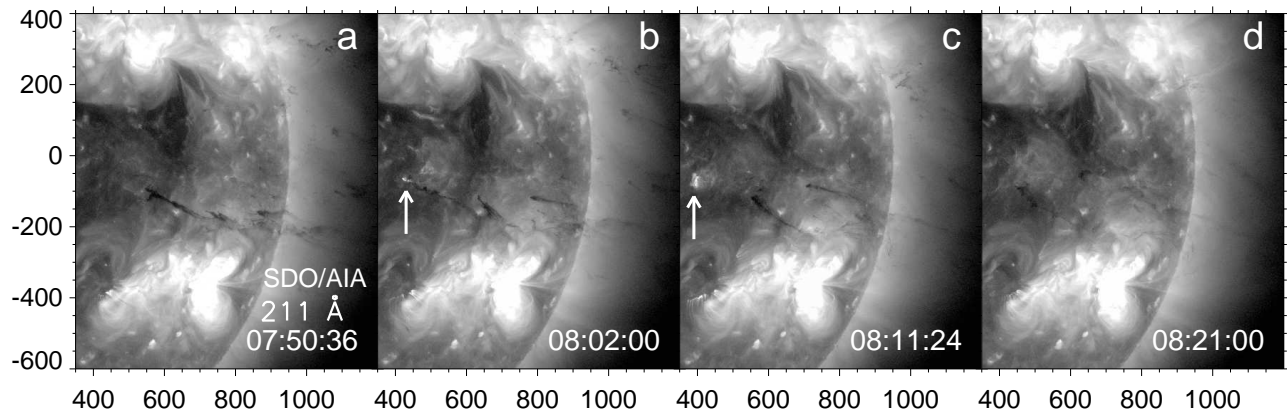


Fig. 8. SDO/AIA 211 Å images of the 2011 June 7 anomalous eruption. The arrows indicate transient brightenings at the places of falling filament fragments.

Most eruptions occur in the ‘normal’ scenario: an eruptive filament expands keeping its magnetic structure. The 2011 December 13 event considered here presents an interesting rare extremity of an isolated negative burst.

Anomalous eruption of a filament with its disintegration appears to evidence reconnection between magnetic fields of the large-scale coronal environment and interior of the filament. In such a case, the signs of the magnetic helicity must not coincide for the ejected magnetic cloud and the active region from which the eruption originated (Uralov et al. 2013). An anomalous eruption presumably occurs if an eruptive filament passes through vicinities of a coronal null point. One of possible scenarios of an event with an anomalous eruption was proposed here.

As shown, parameters of ejected plasma projected onto the solar disk can be estimated from multi-frequency total flux records of negative bursts. Ongoing observations with NoRP and NoRH along with EUV data can shed further light on different scenarios and parameters of solar eruptions and can be used among the factors in forecasting geoeffectiveness of Earth-directed magnetic clouds.

Being associated with eruptions on the Earth-facing solar surface, microwave negative bursts indicate events, in which potentially geoeffective CMEs develop. Especially hazardous can be anomalous eruptions, whereas occurrence of negative bursts in such events is not guaranteed. The most demonstrative example is the anomalous eruption of 2003 November 18 responsible for the strongest geomagnetic storm in last two decades (Grechnev et al. 2013), but a negative burst could not be detected in this event due to ongoing flaring. Similarly, the negative burst on 2003 May 28 was interrupted by a subsequent flare. Microwave imaging observations are very important also in this respect. Importance of anomalous eruptions also calls for such requirements for future radio telescopes as multi-frequency capability at long microwaves with a field of view excessively covering the solar disk.

Acknowledgements. We thank K. Shibasaki, H. Nakajima, and V. Slemzin for fruitful discussions, V. Zandanov and S. Anfinogentov for their assistance in data processing. We are indebted to the anonymous referee for useful remarks. We are grateful to instrumental teams operating Nobeyama solar facilities, SSRT, EIT and LASCO on SOHO (ESA & NASA), USAF RSTN network, STEREO, and SDO missions.

This study was supported by the Russian Foundation of Basic Research under grants 11-02-00757, 12-02-00037, 12-02-33110-mol-a-ved, and 12-02-31746-mol-a; the Integration Project of RAS SD No. 4; the Program of basic research of the RAS Presidium No. 22, and the Russian Ministry of Education and Science under projects 8407 and 14.518.11.7047.

References

Chertok, I. M., & Grechnev V. V. 2003, *Astronomy Reports*, 47, 934
 Chertok, I. M., Grechnev, V. V., Uralov, A. M. 2009,

Astronomy Reports, 53, 355
 Covington, A., & Dodson, H. 1953, *Journal of the Royal Astronomical Society of Canada*, 47, 494
 Delaboudinière, J.-P., Artzner, G. E., Brunaud, J., Gabriel, A. H., Hochedez, J.-F., Millier, F., Song, X. Y., Au, B. et al. 1995, *Sol. Phys.*, 162, 291
 Gilbert, H. R., Alexander, D., Liu, R. 2007, *Sol. Phys.*, 245, 287
 Grechnev, V. V., Lesovoi, S. V., Smolkov, G. Y., Krissinel, B. B., Zandanov, V. G., Altyntsev, A. T., Kardapolova, N. N., Sergeev, R. Y., Uralov, A. M., Maksimov, V. P., Lubyshev, B. I. 2003, *Sol. Phys.*, 216, 239
 Grechnev, V.V., Chertok, I.M., Slemzin, V.A., Kuzin, S.V., Ignat’ev, A.P., Pertsov, A.A., Zhitnik, I.A., Delaboudinière, J.-P., Auchère, F. 2005, *J. Geophys. Res.*, 110, A09S07
 Grechnev, V. V., Uralov, A. M., Slemzin, V. A., Chertok, I. M., Kuzmenko, I. V., Shibasaki, K. 2008b, *Sol. Phys.*, 253, 263
 Grechnev, V. V., Kuzmenko, I. V., Uralov, A. M., Chertok, I. M. 2011a, *Astronomy Reports*, 55, 637
 Grechnev, V. V., Uralov, A. M., Chertok, I. M., Kuzmenko, I. V., Afanasyev, A. N., Meshalkina, N. S., Kalashnikov, S. S., Kubo, Y. 2011b, *Sol. Phys.*, 273, 433
 Grechnev, V. V., Uralov, A. M., Slemzin, V. A., Chertok, I. M., Filippov, B. P., Rudenko, G. V., Temmer, M. 2013, *Sol. Phys.*, doi: 10.1007/s11207-013-0316-6. In press
 Howard, R. A., Moses, J. D., Vourlidas, A., Newmark, J. S., Socker, D. G., Plunkett, S. P., Korendyke, C. M., Cook, J. W. et al. 2008, *Space Sci. Rev.*, 136, 67
 Hyder C. L. 1967a, *Sol. Phys.*, 2, 49
 Hyder C. L. 1967b, *Sol. Phys.*, 2, 267
 Kuz’menko, I. V., Mikhailina, F. A., Kapustin, B. A. 2008, *Radiophysics and Quantum Electronics*, 51, 905.
 Kuzmenko, I., Grechnev, V., Uralov, A. 2009, *Astronomy Reports*, 53, 1039
 Lemen, J. R., Title, A. M., Akin, D. J., Boerner, P. F., Chou, C., Drake, J. F., Duncan, D. W., Edwards, C. G., Friedlaender, F. M., Heyman, G. F. et al. 2012, *Sol. Phys.*, 275, 17
 Maksimov, V. P., & Nefedyev, V. P. 1991, *Sol. Phys.*, 136, 335
 Nakajima, H., Sekiguchi, H., Sawa, M., Kai, K., Kawashima, S. 1985, *PASJ*, 37, 163
 Nakajima, H., Nishio, M., Enome, S., Shibasaki, K., Takano, T., Hanaoka, Y., Torii, C., Sekiguchi, H. et al. 1994, *Proc. IEEE*, 82, 705
 Sawyer, C. 1977, *Sol. Phys.*, 51, 203
 Slemzin, V., Chertok, I., Grechnev, V., Ignat’ev A., Kuzin S., Pertsov A., Zhitnik I., Delaboudinière J.-P. 2004, In A.V. Stepanov, E.E. Benevolenskaya, and A.G. Kosovichev, editors, *Multi-Wavelength Investigations of Solar Activity*, *Proc. IAU Symp.* 223, 533
 Smolkov, G. I., Pistolokors, A. A., Treskov, T. A., Krissinel, B. B., Putilov, V. A. 1986, *Ap&SS*, 119, 1
 Tanaka, H., & Kakinuma, T. 1960, *Proc. Research Institute of Atmospheric, Nagoya Univ., Japan*, 7, 72
 Torii, C., Tsukiji, Y., Kobayashi, S., Yoshimi, N., Tanaka, H., Enome, S. 1979, *Proc. Research Institute of Atmospheric, Nagoya Univ., Japan*, 26, 129
 Uralov, A. M., Grechnev, V. V., Rudenko, G. V., Myshyakov, I. I., Chertok, I. M., Filippov, B. P., Slemzin, V. A.: 2013, *Sol. Phys.*, in preparation
 Yashiro, S., Gopalswamy, N., Michalek, G., St. Cyr, O. C., Plunkett, S. P., Rich, N. B., Howard, R. A. 2004, *J.*

